Next Level Geothermal Power Generation (NGP) – A new sCO_2-based geothermal concept

Robin Sudhoff[1)], **Stefan Glos**[1)], **Michael Wechsung**[1)], **Benjamin M. Adams**[2),3)], **Martin O. Saar**[2),3)]
[1)] Siemens AG, Gas and Power Division, Germany
[2)] ETH Zurich, Geothermal Energy and Geofluids Group, Dept. of Earth Sciences, Switzerland
[3)] CO_2 POWER, Zurich, Switzerland

Keywords: carbon dioxide, CCUS, geothermal energy, alternative cycle, power generation, LCOE

ABSTRACT

Geothermal power generation with supercritical carbon dioxide (sCO_2) has been object of numerous research studies over the past years. In comparison to conventional hydrothermal power plants, CO_2-based geothermal systems exhibit several thermophysical, subsurface and power plant equipment, advantages. Essentially, a more effective geothermal heat extraction and less need for auxiliary pumping power, due to a much stronger thermosiphon effect, compared to water-based geothermal energy extraction can be highlighted. In this paper a thermodynamic evaluation of ‘Next Level Geothermal Power Generation’ (NGP) systems is provided. The impact of scaled geothermal cycles and of deviating geologic and ambient conditions, such as reservoir permeability, depth, temperature gradient and the cooling conditions, on both power output and costs is assessed. Furthermore, an improvement of the thermosiphon effect by an optimized cooling is demonstrated. Based on the thermodynamic simulations, capital costs and levelized costs of electricity (LCOE) are calculated and compared with other technologies. The results show that scaled NGP systems with optimized cooling can generate electricity at competitive LCOE.

1. INTRODUCTION

Carbon dioxide (CO_2) emissions from fossil energy production and the associated increase in atmospheric concentrations have led to a global temperature increase of 1°C in recent decades and will lead to further global warming in the future (IPCC 2018). Therefore, it is necessary to develop electricity systems that reduce the amount of CO_2 emitted into the atmosphere while generating steady, continuous power. To meet the climate goal of limiting the global mean temperature rise to well below 2°C, agreed upon by a majority of nations in the Paris Agreement (United Nations Framework Convention on Climate Change, 2015), CO_2 emissions have to be reduced and eliminated immediately. As not a single technology will make this possible, the necessary reduction in CO_2 emissions must be achieved through several integrated technologies. In the electricity sector, which accounts for 25% of the total CO2 emissions, existing power plants can be retrofitted with CO_2 capture technologies and carbon-neutral power systems can replace existing generation (IPCC 2014; Metz et al. 2005).

CO_2 from existing fossil power plants, cement factories, biofuel refineries, or from other large, stationary sources can be captured, transported and injected into a subsurface reservoir to achieve negative emissions to the atmosphere, resulting in Carbon Capture and Storage (CCS). The CO_2 is permanently stored in the underground in deep saline aquifers or partially depleted oil/gas fields. The vertical leakage of the stored CO_2, which is naturally buoyant at the storage conditions, is contained by an overlying low permeability caprock. Due to the depth of the storage formation, that can be several kilometers, the average reservoir temperatures is higher than the temperature of the injected CO_2, so that the injected CO_2 can extract geothermal heat.

Against this background, the use of sCO_2 as an alternative energy-extraction medium from naturally permeable sedimentary-basin reservoirs and use in direct geothermal power plant applications has been discussed (Randolph and Saar, 2011; Adams et al., 2014; Adams et al., 2015; Garapati et al., 2015).

In addition to sCO_2-based geothermal power, renewable energy sources such as wind and solar can provide energy without associated CO_2 emissions. However, the feed-in of renewables is fluctuating, as the are only producing power if the given resources are available. With increasing shares of wind and solar capacity, energy storage systems are needed to ensure the reliability of the power grid, resulting in additional costs. Large-scale bulk energy storage systems, such as Pumped Hydroelectric (PHES) and Compressed Air (CAES), may not be able to provide the required expanded capacity. In contrast to these energy storage technologies, geothermal energy is widely available and can be accessed by NGP systems.

In this paper, the thermodynamic evaluation of NGP systems is provided in a first step. With the aim of increasing the power output, a scaled wellfield pattern is analysed. Based on the work of Adams et al. (2015), thermodynamic simulations are carried out. The effect of the geologic conditions reservoir depth, permeability and geothermal temperature gradient on power generation is assessed. In a further sensitivity investigation, the influences of the heat sink of the power plant are focussed. Furthermore, the thermosiphon effect is enhanced by an optimized cooling system using subcooling. In a second step, capital costs of scaled NGP system applications are evaluated. The resulting levelized costs of electricity (LCOE) are derived and compared to other renewable and conventional power generation technologies.

2. SYSTEM OVERVIEW

The idea of a NGP system may be summarized as follows: CO_2 from one or several fossil fuel power plants, or other CO_2 emitters like refineries or cement plants, is captured, employing Carbon-Capture (CC) technologies after which the CO_2 can be transported to a NGP site, where it is injected into a geologic storage formation. For NGP, the CO_2 storage formation needs to exhibit a temperature that is sufficiently high to conduct NGP operations economically, i.e., at least about 100°C. These sedimentary or stratigraphic basins need to have sufficient permeability of >10 mD (1 mD = 10^{-15} m^2) and need to be overlain by a caprock of sufficiently low permeability about <0.01 mD to enable efficient CO_2 injectivity into the reservoir through the injection well and to prevent a flow through the caprock, against which the CO_2 pools upwardly. In the reservoir, the CO_2 is geothermally heated and a portion is piped back to the surface power plant, where it is expanded in a turbine, driving a generator and hence producing electricity. After the expansion in the turbine, the CO_2 is condensed/cooled and reinjected into the reservoir. To increase the net power output slightly, a supplementary pump can be used optionally. (Adams et al., 2015). The basic principle of the NGP system is shown in Figure 1. The related thermodynamic changes in the state of the CO_2 cycle are shown in the T-s-diagram in Figure 2.

Tab. 1: reference case assumptions

working fluid:	100 % CO_2
amb. temperature (dry bulb):	15 °C
amb. relative humidity:	70 %
geothermal temp. gradient:	35 K/km
reservoir depth:	3,5 km
permeability:	100 mD
reservoir thickness:	100 m
heat rejection with cooling tower and condenser:	
temp. difference at approach point (cooling tower):	7 K
temp. difference at pinch point (condenser):	3 K

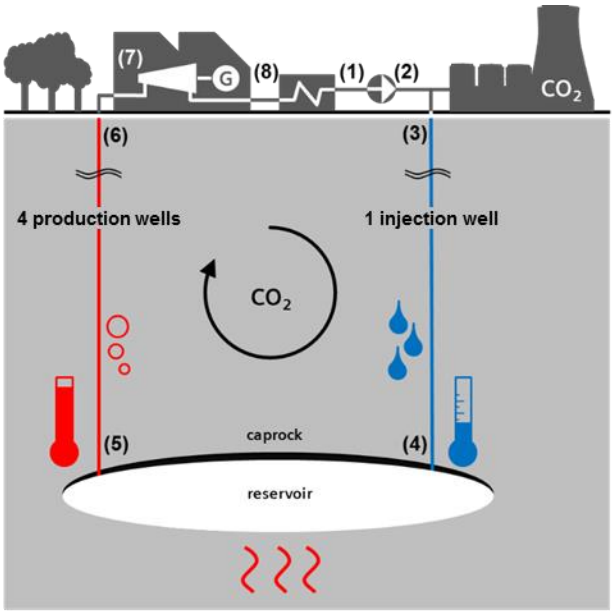

Fig. 1: basic NGP cycle

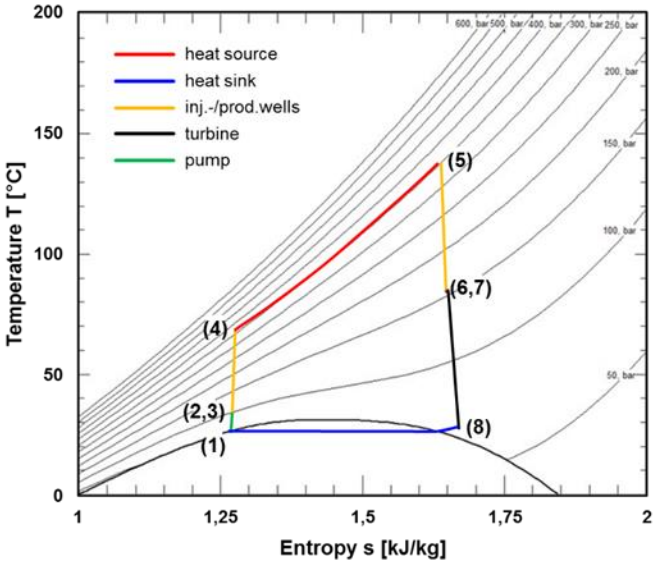

Fig. 2: T-s-diagram of basic NGP cycle

The temperature-dependent density variation and thermal expansibility of sCO_2 is large compared to water. In addition, supercritical CO_2 has a kinematic viscosity that is much lower than that of water under comparable conditions. These two properties result in the formation of a strong thermosiphon, a physical effect which circulates a fluid without the necessity of a mechanical pump. Adams et al. (2014) describes this phenomenon in detail.

3. METHOD

In a basic configuration, injection and production wells are arranged according to a five-spot pattern consisting of one central injection well and four production wells with equal diameters (Randolph and Saar, 2011). The distance between the production wells is 1 km and the footprint is 1 km². This design results in a ratio of 4 production wells per injection well and a ratio of 5 wells per km² footprint. The scaling of the wellfield pattern, shown in Figure 3, is described by assigning a ‘configuration number’ (N), which equals the number of five-spot pattern on a side. The quadratic basic layout is retained.

According to the thermal expansion of sCO_2 within the reservoir the density is reduced. Therefore, a higher number of production wells in order to achieve same flow velocities with same diameters is required. Depending on ambient and reservoir conditions, the ratio of the density at the injection well inlet to the production well inlet is 1.5 to 2.5. More favorable conditions such as a large reservoir depth and good cooling conditions lead to a higher value. By scaling the well pattern, the ‘base case’ ratio of 4 is to be lowered into the given range.

Figure 3 shows the basic and scaled wellfield pattern and the development of both ratios with an increasing configuration number. While the pattern remains unchanged, the production to injection well ratio can be reduced due to the decreasing percentage of edge and corner wells. Furthermore, the scaling significantly reduces the number of required wells per km². This and the use of economies of scale leads to the expectation of lowered capital costs. Bielicki et al. (2017) found that well patterns scaled to N = 5 are most often the cheapest size concerning capital cost and LCOE. Therefore, systems up to size N = 5 are examined.

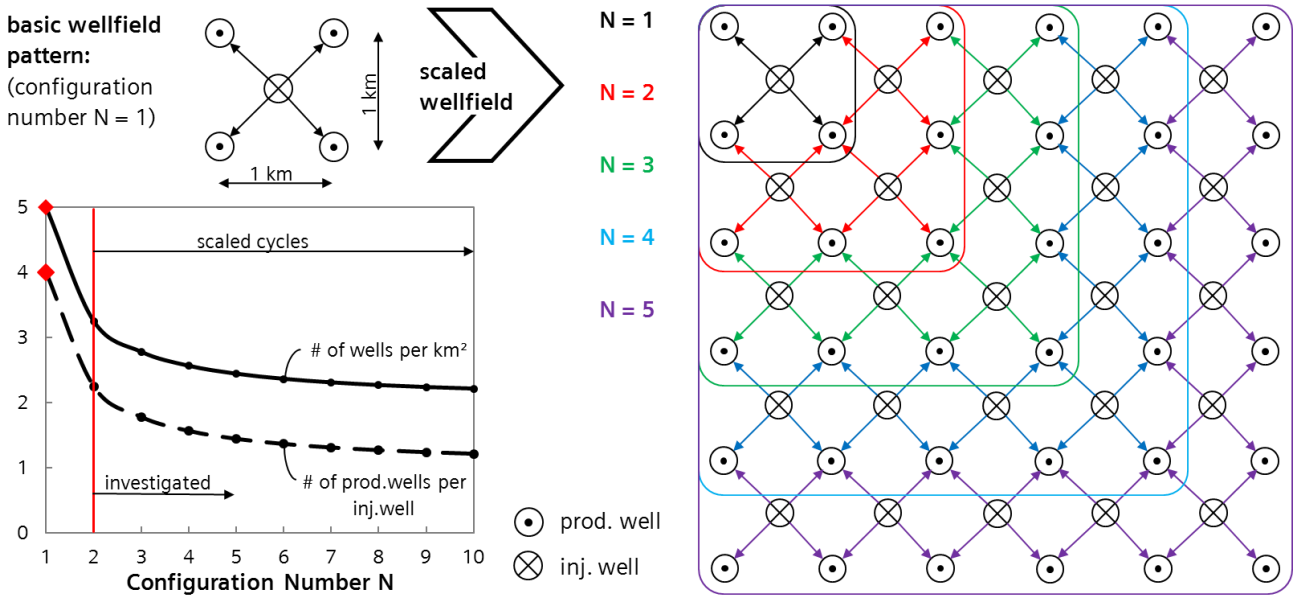

Fig. 3: scaling of wellfield pattern leads to reduced specific number of wells

4. THERMODYNAMIC EVALUATION

4.1 Impact of deviating site conditions

Geothermal power generation depends on the conditions of specific geological formations and surface ambient conditions. The impact of varying reservoir conditions is investigated for a deviation of the cooling system and ambient temperature as well as combinations of reservoir depth, geothermal temperature gradient and permeability and for different well diameters. The results are summarized in Figure 4.

If freshwater cooling can be used instead of a closed cooling circuit with a cooling tower, a lower condensation temperature and turbine outlet pressure is achieved. This increases the turbine output and, due to the better thermosiphon effect, the produced mass flow. Parasitic fan power for a mechanical draft cooling tower is eliminated. The influence of the ambient temperature is lower, since the reservoir temperature also changes with a constant geothermal temperature gradient. Thus, the advantage of heat dissipation at low temperatures is partially counteracted by a lower reservoir temperature.

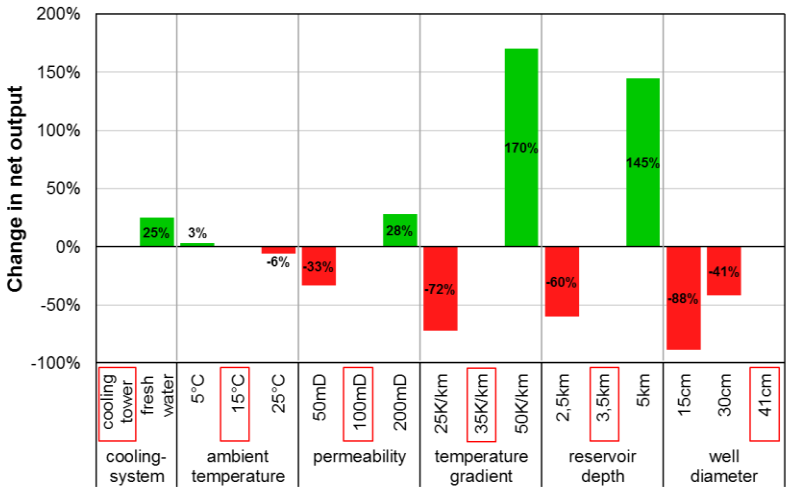

Fig. 4: change in net output for site conditions deviating from reference case assumptions (framed red)

Looking at the geological boundary conditions the power output increases with a higher permeability. The greater the

permeability of the reservoir is, the lower the pressure losses in the reservoir are, so that a larger mass flow can be produced with the same driving pressure difference of the thermosiphon. In addition, the power output rises with increasing temperature gradients, as the driving density difference between the injection and production wells increases and the turbine inlet temperature rises. Both the mass flow and the enthalpy difference along the turbine increase. Furthermore, there is a high effect of the reservoir depth on the net output. With increasing depth, the reservoir temperature increases and intensifies the thermosiphon effect.

In addition, the well diameter also has a large influence on the net output. As an indicator for the diameter determination, the pressure loss in the wells can be compared with the pressure loss in the reservoir. The diameter is chosen so that both loss parameters are approximately the same. For cost optimization, savings from smaller diameters and the reduced revenue from reduced net output due to higher pressure losses must be compared.

4.2 Thermosiphon improvement by optimized cooling

Subcooling is defined as a cooling below the saturation temperature after the condensation of a fluid. It is not useful in conventional water/steam processes. While the mean temperature of the heat absorption and thus the thermal efficiency of the process decreases, the cooling effort and costs of the power plant increase. Due to the low temperature dependence of the density of water, there is no advantage in reducing the compression work of the feed water pump. Only the substance properties of CO_2 in combination with the use of the working medium in geothermal power plants, with the associated overcoming of large geodetic height differences, enables the beneficial use of subcooling.

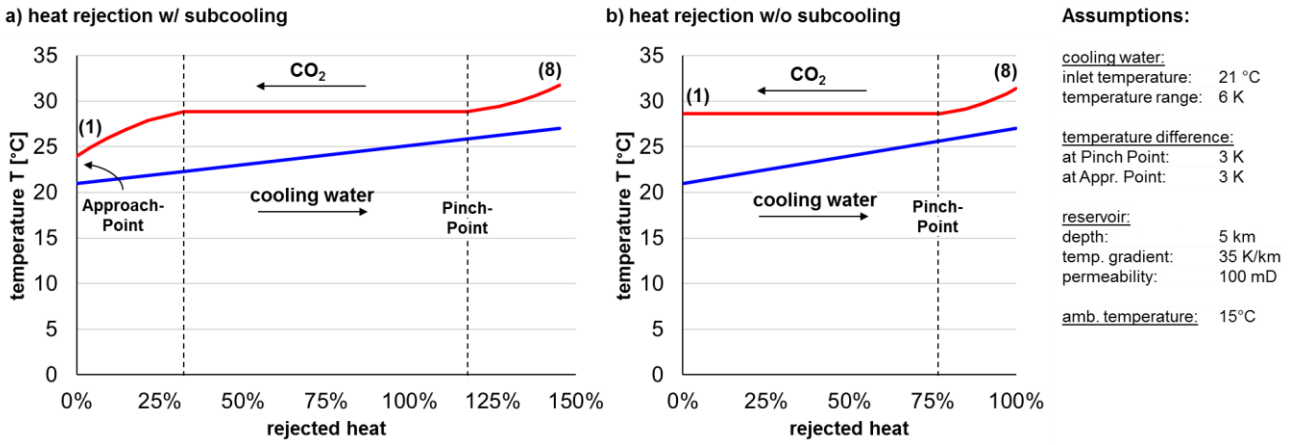

Fig. 5: Comparison of heat rejection with and without subcooling in Q-T-diagram

The Q-T-diagrams in Figure 5 show the temperature of the cold (cooling water) and warm (CO_2) medium along the transferred heat in heat exchangers. In addition to the subcooling unit, the condenser and desuperheater are presented. In the desuperheater, CO_2 is cooled from the supercritical state to the dew line.

The condensation temperature of the working medium is set by the specifications at the pinch point between condenser and desuperheater. To increase the thermosiphon and turbine power output the condensation temperature which is equal to the outlet temperature at state (1) without subcooling (Case b) can only be lowered by better cooling water conditions. With subcooling (Case a) the temperature at state (1) can be reduced independently of the condensation temperature. It is assumed that the temperature differences at approach and pinch point are equal. The turbine outlet pressure is hardly influenced by this.

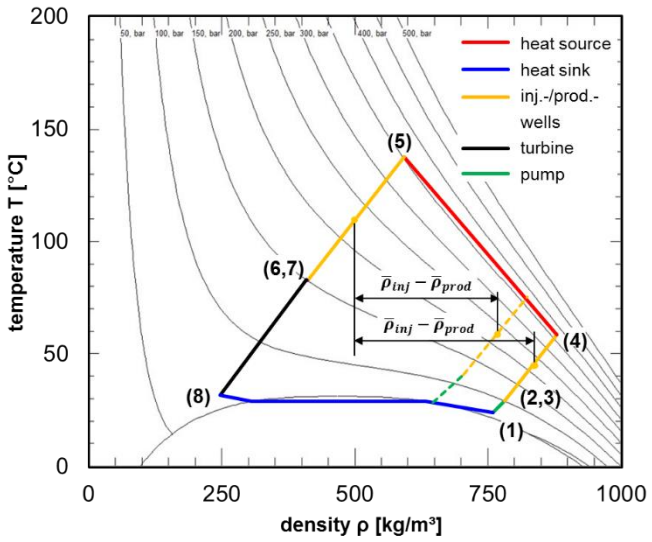

Fig. 6: Comparison of heat rejection with (solid line) and without subcooling (dashed line) in T-ρ diagram

Tab. 2: Operational parameters of both variants (N = 5)

		w/ subcooling	w/o subcooling
turbine outlet pressure (8)	bar	69.9	70.2
temp. at compr. Inlet (1)	°C	24.0°C	28.6°C
average injection density	kg/m³	840	770
compr. pressure increase	bar	31	47
mass flow for max. net output	kg/s	18,500	16,000
net power output ($P_{turbine}$ - P_{pump})	MW	262	184

The reduced temperature leads to an advantage due to the increase in density at the compressor inlet assuming that the reservoir temperature (state 5) is reached in both cases (see Figure 6, Table 2). Consequently, a larger difference between the mean density of the injection and production wells results in a stronger thermosiphon effect. Since the compressor power input of the case with subcooling decreases due to the improved thermosiphon effect, the operation point with maximum power output shifts to higher mass flows.

Regarding component size and costs, in this example, the amount of rejected heat increases by about 45%, of which 60% results from a higher mass flow and 40% from the increased enthalpy difference along heat transfer.

As the power input of the compressor fluctuates depending on the boundary conditions ‘cooling water inlet temperature’ and ‘reservoir depth’, the increase in power, shown in figure 7 below, due to subcooling varies.

Subcooling results in a particularly high relative power increase for low depth reservoirs and for cooling conditions that cause the condensation temperature to be close to the critical temperature of CO_2 ($T_{crit} \approx 31$ °C).

Reasons for this are, firstly, that at low reservoir depths (z = 2.5 km) the difference in mean temperatures between heat input and rejection is small. The thermosiphon effect is

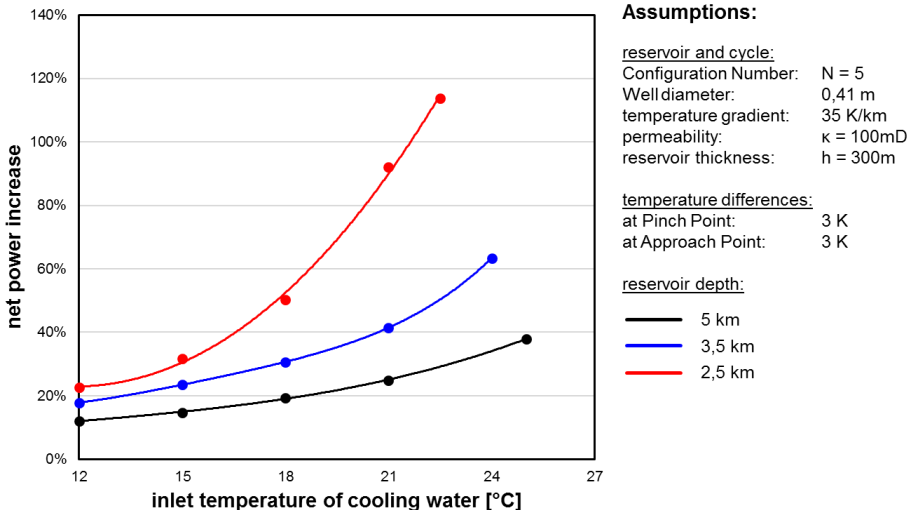

Fig. 7: net power increase due to subcooling depending on cooling water conditions and reservoir depth

smaller compared to reservoirs at greater depths (z = 5 km). Therefore, a reduction of the compressor inlet temperature by subcooling, which leads to an equal improvement of the thermosiphon at both reservoir depths, has a stronger relative influence on the net output at shallow depths. Secondly, the course of isobars in the area of the boiling line near the critical point is flatter than at lower temperatures. Thus, the density is increased more strongly by subcooling at higher cooling water temperatures than at lower temperatures.

5. ECONOMIC EVALUATION

5.1 Capital Cost (CC)

For capital cost modelling purposes, the NGP energy system may be structured in three parts: the reservoir, the surface power plant and surface piping. The calculation of costs for CO_2 capture from industrial or power plant processes is not part of this paper. Furthermore, no revenues or costs for the CO_2 to be stored are taken into account.

Reservoir costs include all activities for wellfield completion such as well drillings. In order to monitor the injection of CO_2, to identify leaks, to verify the reservoir models and to be able to pronounce early warnings in case of disturbances, measures for the observation are necessary. For this purpose, an additional monitor well, which extends to the cap rock, must be planned per each injection or production well. Furthermore, one stratigraphic well per site is required to extract a drill core and determine geological conditions such as porosity and permeability (Ansolobehere et al. 2015). For cost assessment, CO_2 wellfield development and monitor well drilling cost estimates are based on the detailed cost analysis for geologic CO_2 sequestration published by the United States Environmental Protection Agency, EPA (2008). For well drilling estimates the Geothermal Electricity Technology Evaluation Model (GETEM) is used.

The estimated costs associated with the surface power plant include the component costs of the turbine, the turbine train including generator, the pump and the cooling system as well as

- construction costs and costs for small systems (1),
- costs for internal electrical and grid connections and components (2),
- costs for plant design and project management (3) and
- costs for assembly, commissioning and logistics (4)

that are typically within the scope of a turnkey project.

The power plant can be realized by adjusting components which are currently used in combined cycle power plants (CCPP) or steam power plants (SPP). Preliminary calculations, based on Siemens' product portfolio and in-house data show that the main cost drivers are related to the heat rejection, for example cooling tower and heat exchanger. Favourable cooling conditions, for example access to direct cooling at coastal or offshore locations, can therefore lead to significant cost reductions.

The surface piping system connects the wells with the power plant. The costs are 2 million $/(m·km), multiplied by the diameter and length of each piece of piping [EPA 10]. Because the pressure in the piping varies depending on reservoir conditions, environmental conditions, and pipeline position, the influence of different wall thicknesses is taken into account.

Table 2 summarizes the geologic properties of the reservoirs, the thermal boundary conditions of the power plant and the most relevant thermodynamic assumptions and characteristics for considered sites. During the assumed operation lifetime of 25 years, no thermal depletion of the reservoirs was assumed.

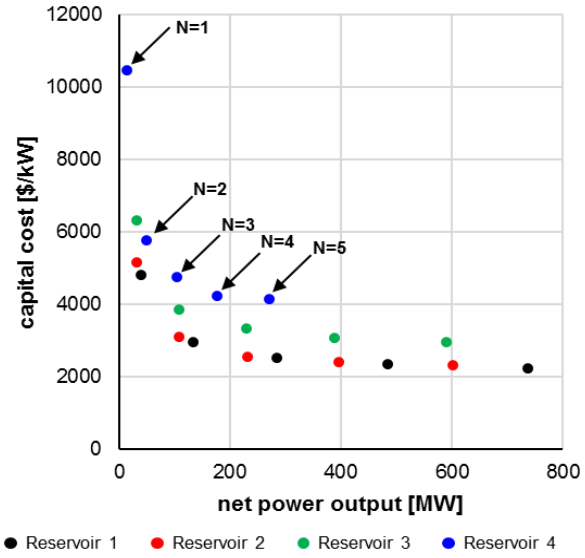

Fig. 8: Decrease of capital costs for scaled cycles

Tab. 2: Boundary conditions of example reservoirs

		res. 1	res. 2	res. 3	res. 4
depth	km	5	3.5	5	3.5
Temp. gradient	K/km	35	50	35	35
permeability	mD	200	100	200	100
thickness	m	100	100	100	200
amb. temperature	°C	10	10	15	5
cooling type	-	fw	ct	ct	ct

General Assumptions:
supplemental pumping considered
well diameter: 0.41 m
temp. difference at Pinch and Approach Point (HX): 3 K
temp. difference at Approach Point (cooling tower): 7 K
capacity factor: 0.9

fw: freshwater cooling, ct: cooling tower

The presentation of capital costs in Figure 8 shows that the greatest savings can be achieved by scaling from N = 1 to N = 2. For the four example reservoirs examined, this is on average 40 %. By scaling to the coordination number N = 3, the value of costs is reduced by 50% from N = 1. Less significant cost reductions can be achieved by an additional scaling beyond the coordination number N = 3.

Figure 9 shows comparative values for the specific investment costs of different alternative and conventional technologies and power plant types, as well as the results of this work for the coordination numbers N = 1 to 5 and different reservoir conditions. It should be noted that some examples, such as photovoltaics and wind energy, are not base-load-capable or plannable, so that additional costs for energy storage must be considered for a comparison. Furthermore, the emission of CO_2 and other substances harmful to the climate and health in gas-fired or coal-fired power plants results in additional costs for compliance with environmental regulations. Therefore, solar thermal power plants with storage, conventional geothermal power plants and nuclear power plants are suitable as base load-capable and CO_2-free technologies for comparative values.

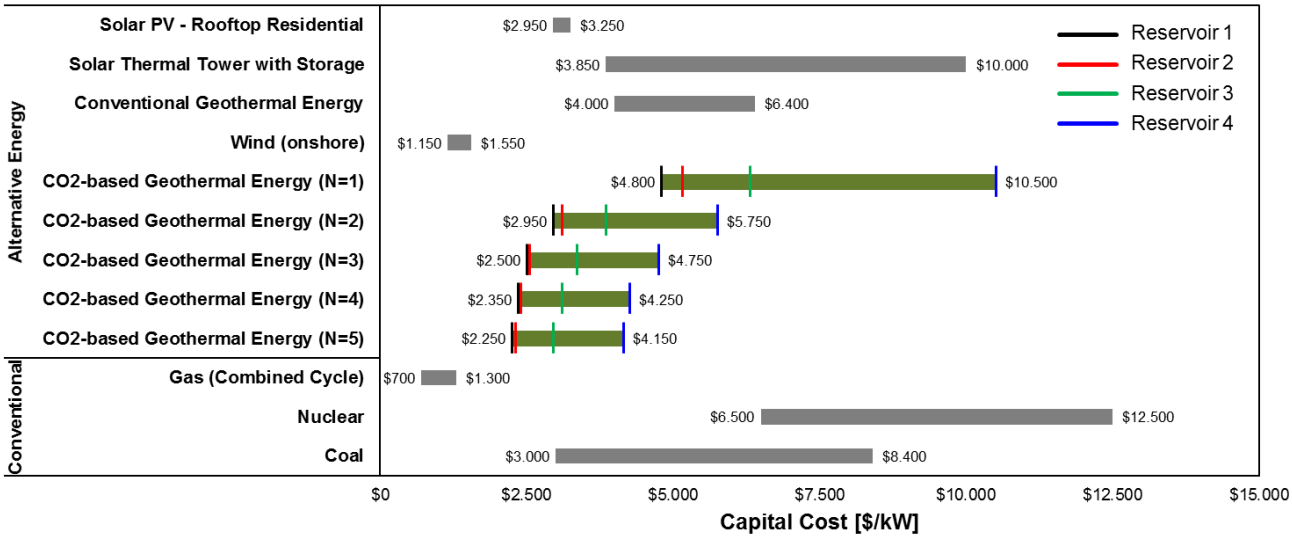

Fig. 9: Capital Cost comparison for various alternative and conventional Power Plants

5.2 Levelized Cost of Electricity (LCOE)

The calculation of the Levelized Costs of Electricity (LCOE) is based on a comparison of all costs that arise over the lifetime of a power plant from construction to the end of operation as well as the total amount of energy generated over its operating lifetime. As the present values of revenues in the future have a lower value than current revenues, the net present value method is used to calculate all cash flows and the annual quantity of electricity produced by discounting them to a common reference point. This calculates an electricity price that leads to a net present value of the asset of zero at the end of the lifetime. (Kost et al. 2018, VGB 2015)

$$NPV = \sum_{t=1}^{n} \frac{LCOE \cdot M_{t,el} - (I_t + A_t)}{(1+i)^t} = 0 \qquad (1)$$

NPV: net present value, t: year of operation time, n: operation time, $M_{t,el}$: electricity produced in year t
I_t: Investment costs in year t, A_t: operation costs in year t, i: weighted average cost of capital

To evaluate the economic competitiveness of an NGP power plant, the LCOE can be compared. The calculation is based on assumptions and financial boundary conditions following Lazard's latest comparative LCOE analysis (Lazard, 2018 - Table 3).

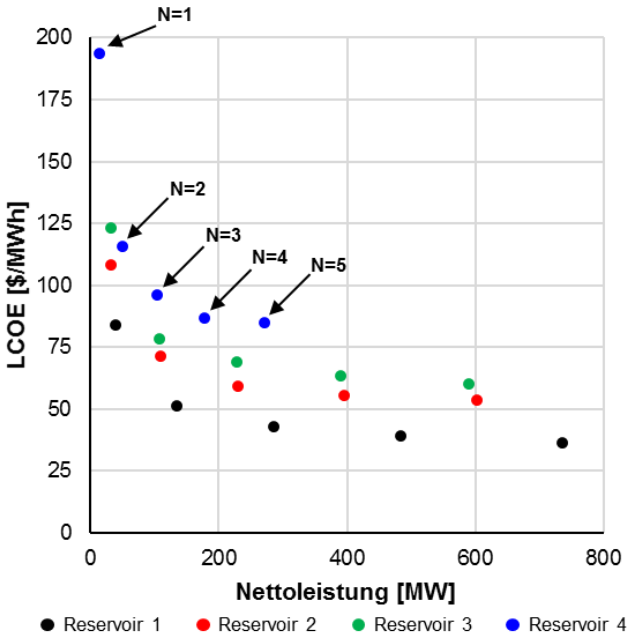

Fig. 10: Decrease of LCOE for scaled cycles

Tab. 3: financial and regulative boundary conditions of LCOE calculation

capacity factor	90 %
operation lifetime	25 years
Project development/ construction time	1 year
annual O&M costs	80 - 425 $/kW·a
O&M cost escalation rate	2.25%
Equity rate	40%
Cost of equity	12%
Cost of debt before tax	8%
Combined tax rate	40%
Depreciation schedule	Modified accelerated cost recovery system (MACRS) 5-years

Considering the boundary conditions and assumptions presented, Figure 11 shows that an NGP power plant can be operated competitively. The calculated LCOE are within the range typical for other baseload-capable power plants such as coal, nuclear or solar thermal towers, the latter with energy storage.

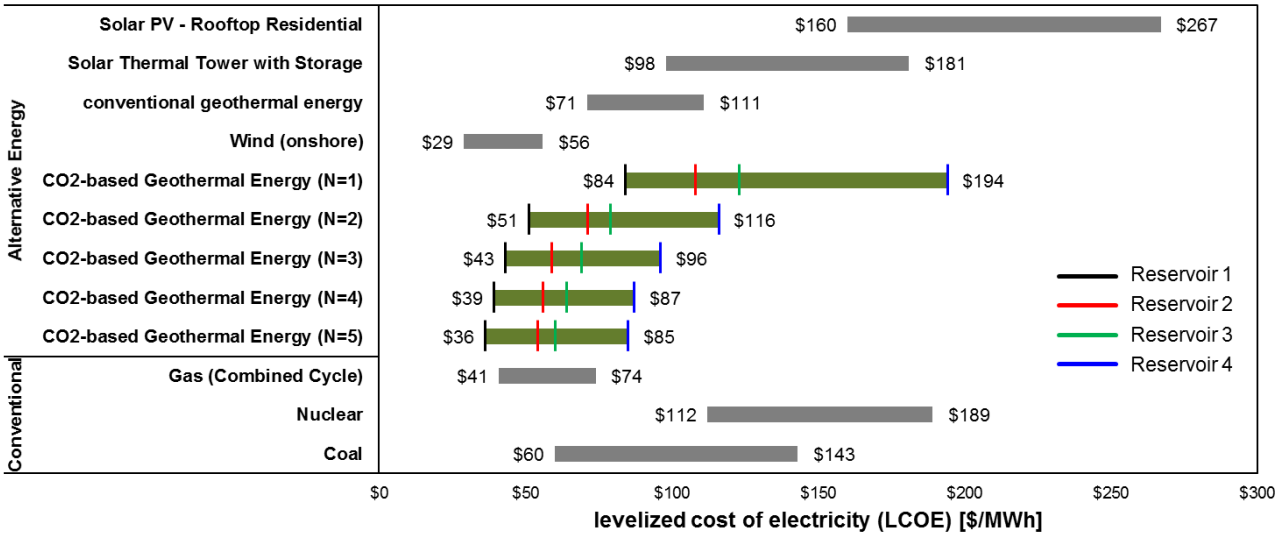

Fig. 11: LCOE comparison for various alternative and conventional Power Plants

6. CONCLUSION

The comparison with other fully dispatchable and emission-free power plant technologies based on the economic indicators provides an indication that geothermal power plants based on supercritical CO_2 with suitable geologic properties can be operated at competitive costs in scaled systems and with optimized cooling, even when a greenfield approach is used.

Scaling the well pattern from the base arrangement on a surface area of one square kilometre (N = 1) to patterns with equal well spacing of up to 25 square kilometres (N = 5) leads to a significant decrease of the LCOE of the plant. The number of wells per area can be reduced as production mass flow increases. Furthermore, economies of scale can be achieved in the component costs of the power plant.

By additional subcooling after the condensation of CO_2 the power output is significantly increased. The driving pressure difference rises with increasing density difference of the CO_2 between injection and production along the geodetic height difference of the wells. Thus, the amount of circulating working medium, depending on the strength of the thermosiphon effect, can be raised.

In the next step, the cost model should be validated and further improved, and the overall business case should be evaluated. Costs for CO_2 capture in a power plant including the following efficiency losses as well as revenues from certificate trading would then be considered.

SOURCES

ADAMS, B.M., KUEHN, T.H., BIELICKI, J.M., RANDOLPH, J.B., & SAAR, M.O.: A comparison of electric power output of CO_2 Plume Geothermal (CPG) and brine geothermal systems for varying reservoir conditions, *Applied Energy* 140, 265-377 (2015)

ADAMS, B.M., KUEHN, T.H., BIELICKI, J.M., RANDOLPH, J.B., & SAAR, M.O.: On the importance of the thermosiphon effect in CPG (CO_2 Plume Geothermal) power systems, *Energy* (2014).

ANSOLOBEHERE, S., J. BEER, J. DEUTCH, A.D. ELLERMAN, J. FRIEDMAN, H. HERZOG, H. JACOBY, P. JOSCOW, G. McRAE, R. LESTER, E. MONIZ and E. STEINFELD: The Future of Coal: Options for a Carbon-Constrained World, an interdisciplinary MIT study. *MIT Interdisciplinary Study Report*, Massachusetts Institute of Technology, Cambridge, MA (http://globalchange.mit.edu/publication/14536) (2007)

BIELICKI, J.M., ADAMS, B.M., CHOI, H., JAMIYANSUREN, B., TAFF, S.J., BUSCHECK, T.A., OGLAND-HAND, J.D., RANDOLPH, J.B. and SAAR, M.O.: Cost-Competitive Geothermal Electricity from Geologic CO2 Storage, *Energy Conversion and Management* (2017)

EPA (United States Environmental Protection Agency): Geologic CO_2 Sequestration Technology and Cost Analysis, *Technical support document* (2008)

GARAPATI, N., RANDOLPH, J.B. & SAAR, M.O.: Brine displacement by CO_2, energy extraction rates, and lifespan of a CO_2-limited CO_2 Plume Geothermal (CPG) system with a horizontal production well, *Geothermics*, doi.org/10.1016/j.geothermics.2015.02.005, 55:182–194, (2015).

IPCC (Intergovernmental Panel on Climate Change): Climate Change 2014: Mitigation of Climate Change. Working Group III Contribution to the Fifth Assessment Report of the Intergovernmental Panel on Climate Change. Working Group III Contribution to the Fifth Assessment Report of the Intergovernmental Panel on Climate Change. Cambridge: Cambridge University Press. doi:10.1017/CBO9781107415416 (2014)

IPCC (International Panel on Climate Change): Global Warming of 1.5°C. An IPCC Special Report on the impacts of global warming of 1.5°C above pre-industrial levels and related global greenhouse gas emission pathways, in the context of strengthening the global response to the threat of climate change, sustainable development, and efforts to eradicate poverty [Masson-Delmotte, V., P. Zhai, H.-O. Pörtner, D. Roberts, J. Skea, P.R. Shukla, A. Pirani, W. Moufouma-Okia, C. Péan, R. Pidcock, S. Connors, J.B.R. Matthews, Y. Chen, X. Zhou, M.I. Gomis, E. Lonnoy, T. Maycock, M. Tignor, and T. Water-field (eds.)]. In Press. 2018

KOST, C., SHAMMUGAM, S., JÜLCH, V., NGUYEN, H., SCHLEGL, T.: Stromentstehungskosten erneuerbare Energien, Fraunhofer-Institut für Solare Energiesysteme ISE, 2018

LAZARD: Lazard's Levelized Cost of Energy Analysis – Version 12.0, retrieved from https://www.lazard.com (2018)

METZ, B., DAVIDSON, O., de CONINCK, H., LOOS, M., & MEYER, L.: Carbon Dioxide Capture and Storage. Intergovernmental Panel on Climate Change (Vol. 2). doi:10.1002/anie.201000431 (2015)

MINES, G.: GETEM User Manual, retrieved from https://www.energy.gov (2016)

RANDOLPH, J.B., & SAAR, M.O.: Combining geothermal energy capture with geologic carbon dioxide sequestration, *Geophysical Research Letters*, doi.org/10.1029/2011GL047265, 38, L10401, (2011).

VGB PowerTech e.V.: Levelized Cost of Electricity, *Verlag technisch-wissenschaftlicher Schriften*, Essen 2015

Siemens AG, Rheinstraße 100, 45478 Mülheim an der Ruhr
robin.sudhoff@siemens.com